

Trends in the Carbonyl Core (C 1s, O 1s) $\rightarrow \pi^*_{\text{C=O}}$ Transition in the Near-Edge X-ray Absorption Fine Structure Spectra of Organic Molecules

S. G. Urquhart^{*,†} and H. Ade[‡]

Department of Chemistry, University of Saskatchewan, Saskatoon, Saskatchewan S7N 5C9, Canada, and
Department of Physics, North Carolina State University, Raleigh, North Carolina 27695

Received: January 20, 2002; In Final Form: May 28, 2002

Carbonyl core (C 1s, O 1s) $\rightarrow \pi^*_{\text{C=O}}$ transitions are distinctive in the near-edge X-ray absorption fine structure (NEXAFS) spectra of species containing carbonyl groups. These features are used for the chemical microanalysis of organic materials using X-ray microscopy. We have explored the chemical sensitivity of these features in C 1s and O 1s NEXAFS spectra for a series of polymers containing the carbonyl group in a range of different bonding environments. Ab initio calculations are used to explain the origin of the observed trends and to explore the effect that orbital interactions have on the energy of these core (C 1s, O 1s) $\rightarrow \pi^*_{\text{C=O}}$ features. The differences between the experimental and the calculated carbonyl core (C 1s, O 1s) $\rightarrow \pi^*_{\text{C=O}}$ transition energies are systematic and can be used to develop a semiempirical method for predicting the absolute (experimental) transition energies from the calculated transition energies. This relationship is applied to a large body of calculated transition energy data to prepare correlation diagrams for the carbonyl (C 1s, O 1s) $\rightarrow \pi^*_{\text{C=O}}$ transitions. These correlation diagrams will be useful for the analytical application of NEXAFS spectroscopy to organic materials.

1. Introduction

Measuring chemical composition at high spatial resolution is important for studies of many natural, synthetic, and technologically important materials. Such measurements are particularly challenging for organic materials. The combination of high chemical specificity and high spatial resolution is elusive and radiation damage can be severe for many high-energy techniques. The combination of the chemical sensitivity of near-edge X-ray absorption fine structure (NEXAFS) spectroscopy and the high spatial resolution of X-ray microscopy has excellent potential to characterize organic materials at fine spatial scales.¹ Examples of NEXAFS microanalysis include the chemical characterization of polymers,^{1,2} meteorites³ and interplanetary dust particles,⁴ eocene and recent wood,^{5,6} coal, coke, and other organic geological materials,⁷ humic and other soil substances,⁸ and organic lubrication materials in magnetic storage devices.⁹ NEXAFS spectroscopy can be used for quantitative measurement of chemical composition when the chemical components are well understood and suitable spectroscopic models exist.²

The chemical sensitivity of NEXAFS spectroscopy is also extensively used for chemical and structural analysis of surfaces,¹⁰ both with and without spatial resolution. In many of the above studies, some knowledge of the sample's origin, processing, and history was used to interpret the NEXAFS spectra or to select suitable model compounds for spectroscopic comparison. In many cases, the origin and history of a sample may be unknown or subject to conjecture, and therefore NEXAFS spectroscopy by itself may provide the only chemical information for a microscopic domain. In this as well as more common scenarios, a detailed understanding of the structure—

spectral relationships for NEXAFS spectroscopy is essential for chemical microanalysis.

The chemical sensitivity of NEXAFS spectroscopy for organic materials has been explored through an extensive literature of experimental and computational studies.^{11,10} Specific studies of the NEXAFS spectra of polymers have been published by Kikuma et al.,¹⁰ Unger et al.,¹¹ and Ade et al.¹ When NEXAFS spectra are used for chemical analysis, the narrower core $\rightarrow \pi^*$ transitions are often the most useful since they are easier to identify at lower concentrations and signal levels. The chemical sensitivity of these core $\rightarrow \pi^*$ transitions is revealed through chemical shifts in their energies. An example is the resolution of urea and urethane linkages in polyurethanes, which are distinguished through the ~ 0.6 eV shift in the energy of the carbonyl C 1s (C=O) $\rightarrow \pi^*_{\text{C=O}}$ transition.^{12,13}

In this study, we focus on the chemical sensitivity and analytical utility of the carbonyl core (C 1s, O 1s) $\rightarrow \pi^*_{\text{C=O}}$ transitions. The C 1s and O 1s NEXAFS spectra of a series of polymers containing the carbonyl group in a range of different bonding environments are presented. Ab initio calculations were performed to determine the origins of this sensitivity and the role of π^* -delocalization on the carbonyl core (C 1s, O 1s) $\rightarrow \pi^*_{\text{C=O}}$ transitions. The transition energies provided directly from ab initio calculations cannot be used for chemical analysis as the differences between calculation and experiment are as large as the total range of NEXAFS chemical shifts. However, the differences between the calculated and the experimental energy scales are systematic. We have explored these systematic differences and have developed a semiempirical method to predict the absolute (experimental) carbonyl core (C 1s, O 1s) $\rightarrow \pi^*_{\text{C=O}}$ transition energies from the ab initio calculations. Using a large body of calculated carbonyl core (C 1s, O 1s) $\rightarrow \pi^*_{\text{C=O}}$ transition energies, we have created a *spectroscopic correlation diagram* for the carbonyl (C 1s, O 1s) $\rightarrow \pi^*_{\text{C=O}}$ transitions for organic species. This table summarizes the

* Corresponding author. Fax: 306-966-4630. E-mail: stephen.urquhart@usask.ca.

[†] University of Saskatchewan.

[‡] North Carolina State University.

SCHEME 1: Polymer Structures

Polymer Polycarbonate (PC)	
Polyurethane (PUret)	
Polyurea (PUrea)	
Poly(ethylene succinate) (PES)	
Poly(methyl methacrylate) (PMMA)	
Nylon 6 (N6)	
Poly(ethylene terephthalate) (PET)	
Poly(vinyl methyl ketone) (PVMK)	

expected energies for the carbonyl C 1s $\rightarrow \pi^*_{C=O}$ transition and will be a valuable tool for analytical applications of NEXAFS spectroscopy and microscopy to organic materials.

2. Experimental Section

A series of polymers containing the carbonyl group examined in this study are identified in Scheme 1. Samples of poly(vinyl methyl ketone) (PVMK) and poly(ethylene succinate) (PES) were obtained from Scientific Polymer Products, poly(methyl methacrylate) (PMMA) from Aldrich Chemical, and Nylon-6 (N6) from AlliedSignal. The polyurethane (PUret) and polyurea (PUrea) samples were provided by Dow Chemical and have been described previously.¹³ The preparation of poly(ethylene terephthalate) (PET) and polycarbonate (PC) samples was described in Coffey et al.¹⁴ Thin films of PES were prepared by solvent casting from chloroform and floated onto TEM grids. Otherwise, thin polymer sections for C 1s transmission spectroscopy (~ 100 nm thick) were prepared by ultramicrotomy, by using a LKB Nova microtome or a Reichert-Jung Ultracut S cryo-ultramicrotome, and were mounted on standard TEM grids. Thin polymer films for O 1s total electron yield (TEY) spectroscopy were prepared by spin-casting of polymer solutions onto gold-coated silicon wafers. Toluene was used to dissolve PMMA, chloroform was used to dissolve PC, PVMK, and N6, and hexafluoro-2-propanol was used to dissolve PET. The sample thickness was approximately 100 nm, as estimated from the interference colors of the spun-cast films.

The C 1s NEXAFS spectra were acquired with the SUNY@ Stony Brook scanning transmission X-ray microscope (STXM), located at beamline X1A at the National Synchrotron Light Source.¹⁵ Monochromator slits resulting in an energy resolution of ~ 100 – 140 meV were utilized. The imaging ability of the X-ray microscope was used to identify uniform, thin (~ 50 to 200 nm), and continuous regions of the polymer film. Suitable sample regions were needed to minimize spectral distortions arising from pinholes in the sample and from higher order spectral radiation. We did not explicitly test for polarization

dependence, although this could affect the relative intensity of features in the spectra.¹⁰ Normalization (I_0) was achieved by acquisition of spectra through an open hole in the samples. The C 1s spectra were very carefully calibrated. CO₂ gas was added to the He purge in the microscope and the transmission spectrum of the mixture of each polymer and CO₂ gas was recorded.¹⁶ The energies of the CO₂ \rightarrow Rydberg transitions from the high-resolution NEXAFS spectra of Ma et al.¹⁷ were used to calibrate these spectra. The energy scale linearity of this beamline has been established by the X1A beamline personal by using the 1 s transitions of oxygen and nitrogen, as well as the zero order of the grating.

The O 1s NEXAFS spectra of the polymers were acquired with the spherical grating monochromator (SGM) of the Canadian Synchrotron Radiation Facility (CSRF) at the Synchrotron Radiation Center (University of Wisconsin–Madison). These spectra were recorded by total electron yield (TEY). These spectra were normalized to an I_0 spectrum previously measured for a clean piece of Au-coated silicon (which provides a good estimate of the monochromator function) and to the decay in the beam intensity. Monochromator slits were set to provide an energy resolution of ~ 0.2 eV at the O 1s edge. The O 1s spectra were calibrated by setting the energy of the O 1s $\rightarrow \pi^*_{C=O}$ transition in PET to 531.5 eV, based on the energy of this transition in the molecular model dimethyl terephthalate (D3 in Scheme 2).¹⁸

3. Calculations

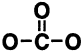
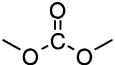
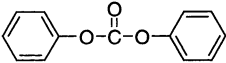
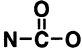
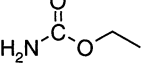
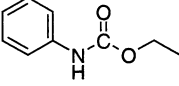
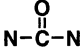
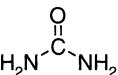
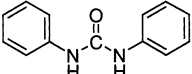
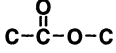
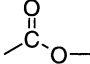
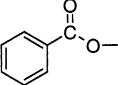
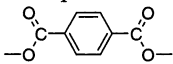
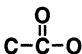
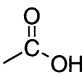
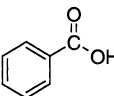
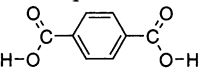
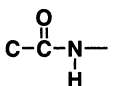
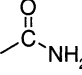
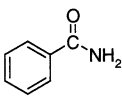
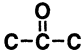
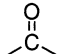
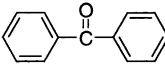
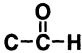
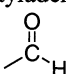
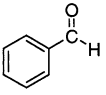
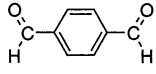
Ab initio calculations were performed for a wide range of different molecular molecules. Core (C 1s, O 1s) ionization potentials and the term values and oscillator strengths for the core (C 1s, O 1s) $\rightarrow \pi^*_{C=O}$ transitions were calculated for these molecules with Kosugi's GSCF3 package.¹⁹ These calculations are based on the improved virtual orbital approximation (IVO), which explicitly takes into account the effect of the core hole in the Hartree–Fock Hamiltonian²⁰ and is highly optimized for calculation of core excited states.¹⁹

The molecular models used for these calculations are presented in Scheme 2. These models are based on simple motifs for the carbonyl group in a range of different bonding environments, from carbonate (A) to aldehyde (H). A series of simple aliphatic models and more complex aromatic substituted models based on these motifs were explored, all corresponding to known molecules (labeled as A1, A2, B1, etc in Scheme 2). Ab initio geometry optimization calculations were performed at the 6-31G* level using the program GAMESS²¹ to provide the molecular structures used in the GSCF3 calculations.

GSCF3 calculations were performed by using the Gaussian-type extended basis set of Huzinaga et al.:²² (621/41) contracted Gaussian-type functions were used on the heavy atoms (C, N, and O); (41) was used on H, and a higher quality basis set (411121/3111/*) was used on the heavy atom onto which the core hole is placed. This basis set generates high-quality predictions of the NEXAFS spectra, while being simple enough to be used for larger molecules. Simulated spectra were generated from these calculations by using a 0.2-eV-wide Gaussian line shape for each calculated core excitation. Only the core $\rightarrow \pi^*_{C=O}$ transitions are considered. The simulated spectra are set to a calculated experimental scale by setting the zero of the calculated term value scale ($\epsilon = 0$) to the calculated (Δ SCF) ionization potential.

Ab initio calculations of models for the C 1s NEXAFS spectra of polycarbonate (PC),²³ poly(ethylene terephthalate) (PET),^{18,23} polyurea (PUrea), and polyurethane (PUret)² have been reported

SCHEME 2: Molecular Structures Used in *ab Initio* Calculations

Motif	Aliphatic	Aromatic	
A: Carbonate 	A1: Dimethyl Carbonate 	A2: Diphenyl carbonate 	
B: Carbamate 	B1: Ethyl Carbamate 	B2: Ethyl N-Phenyl carbamate 	
C: Urea 	C1: Urea 	C2: Diphenyl urea 	
D: Acetate 	D1: Methyl acetate 	D2: Methyl benzoate 	D3: Dimethyl terephthalate 
E: Carboxyl 	E1: Acetic acid 	E2: Benzoic acid 	E3: Terephthalic acid 
F: Amide 	F1: Acetamide 	F2: Benzamide 	
G: Ketone 	G1: Acetone 	G2: Benzophenone 	
H: Aldehyde 	H1: Acetylaldehyde 	H2: Benzaldehyde 	H3: Terephthalaldehyde 

previously. Static Exchange (STEX) calculations on a series of compounds containing the ketone group (similar to our model G) were reported by Yang et al.^{24,25} Our results are similar except for small differences, which we attribute to differences in the basis set chosen. Density functional calculations for the C 1s NEXAFS spectrum of the carbonyl functional group in formic acid, its fluorinated derivatives, and a range of metal carbonyls have been reported by Stener et al.²⁶ We have repeated these calculations here in order to compare the results of these calculations without basis set differences.

4. Results and Discussion

4.1. NEXAFS Spectra of Carbonyl-Containing Polymers.

The C 1s NEXAFS spectra of a series of carbonyl-containing polymers are presented in Figure 1. The chemical structures of these polymers are presented in Scheme 1 and the energies of the carbonyl C 1s $\rightarrow \pi^*_{\text{C=O}}$ transition for these polymers are listed in Table 1.

Features in these C 1s NEXAFS spectra include a band of C 1s (C-H) $\rightarrow 1\pi^*_{\text{C=C}}$ transitions near 285–286 eV. These are characteristic of C=C unsaturation, in this case for the phenyl groups present in PC, PUrea, Puret, and PET. The band at 286–287 eV in the spectrum of PC, Puret, and PUrea is assigned to

the C 1s (C-R) $\rightarrow 1\pi^*_{\text{C=C}}$ transition characteristic of functionalized aromatic groups.¹² At higher energies, generally above 288 eV, broad C 1s $\rightarrow \sigma^*$ transitions are present. We will not discuss these higher energy transitions further as they are less useful for chemical speciation than the sharper core $\rightarrow \pi^*$ transitions.

The carbonyl C 1s $\rightarrow \pi^*_{\text{C=O}}$ transition for each polymer is identified by a line in Figure 1. The magnitude of the shift in energy of these transitions is remarkable: 3.8 eV between polycarbonate (PC) and poly(vinyl methyl ketone) (PVMK). We can correlate the energy of this transition with the identity of the atoms bonded to the carbonyl carbon atom (i.e. $X_1\text{-CO-}X_2$): highest for $X_{1,2}$ = oxygen, lowest for $X_{1,2}$ = carbon, with $X_{1,2}$ = nitrogen intermediate (i.e., O > N > C). The dominant cause of these shifts is likely the inductive effect of the neighboring atoms on the carbonyl C 1s binding energy. Calculations to explore the origin of this shift will be discussed below.

The O 1s NEXAFS spectra of a series of carbonyl containing polymers are presented in Figure 2. The chemical structures of these polymers are presented in Scheme 1 and the energies of the O 1s $\rightarrow \pi^*_{\text{C=O}}$ transitions in these polymers are listed in Table 1. These spectra are dominated by the O 1s (C=O) \rightarrow

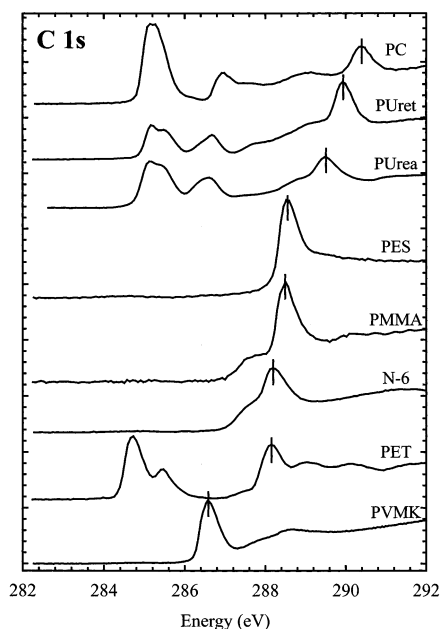


Figure 1. C 1s NEXAFS spectra of polycarbonate (PC), polyurethane (PUret), polyurea (PUrea), poly(ethylene succinate) (PES), poly(methyl methacrylate) (PMMA), nylon-6 (N6), poly(ethylene terephthalate) (PET) and poly(vinyl methyl ketone) (PVMK). Structures of these polymers are presented in Scheme 1.

TABLE 1: Experimental Carbonyl Core (C 1s, O 1s) $\rightarrow \pi^*_{C=O}$ Transition Energies for a Series of Polymers

polymer		C 1s energy, ^a eV _a	O 1s energy, ^b eV
PC	polycarbonate	290.4	532.9
PUret	polyurethane	289.9	N/A
PUrea	polyurea	289.5	N/A
PES	poly(ethylene succinate)	288.6	532.2
PMMA	poly(methyl methacrylate)	288.5	532.1
N6	nylon-6	288.2	532.2
PET	poly(ethylene terephthalate)	288.15	531.5
PVMK	poly(vinyl methyl ketone)	286.6	531.3

^a Calibration: Energy scales were determined by simultaneously measuring the C 1s spectrum of the polymer and CO₂ (admixed with He in the microscope enclosure). The C 1s $\rightarrow 3p(\nu=0)$ Rydberg peak at 294.96 eV¹⁷ was used to calibrate these spectra. ^b Calibration: Energy scales for all polymers were based on the shift required to set the energy of the O 1s $\rightarrow \pi^*_{C=O}$ transition in PET to 531.5 eV, based on the energy of this transition in the molecular model dimethyl terephthalate.¹⁸ As spectra were acquired in different injections over several days, a relative error as large as 0.1 eV may exist in these data.

$\pi^*_{C=O}$ transitions, identified by the line in Figure 2. The trend in the O 1s (C=O) $\rightarrow \pi^*_{C=O}$ transition is similar to the trend in the carbonyl C 1s $\rightarrow \pi^*_{C=O}$ series, except that the relative order of the N6 and the PMMA $\pi^*_{C=O}$ energies is reversed and that the overall energy difference between the core $\rightarrow \pi^*_{C=O}$ transition in PVMK and PC is smaller at the O 1s edge (1.6 eV) than at the C 1s edge (3.8 eV).

In polymers with two chemically inequivalent oxygen sites (PC, PES, and PET), there is also an O 1s (O–R) $\rightarrow \pi^*_{C=O}$ transition at slightly higher energy (534–536 eV). This transition arises from delocalization of the $\pi^*_{C=O}$ density onto the –OR oxygen site.¹⁸ O 1s $\rightarrow \sigma^*_{C-O}$ and O 1s $\rightarrow \sigma^*_{C=O}$ transitions are present at higher energy, but will not be discussed further.

4.2. Ab Initio Calculations. Ab initio calculations were performed to study the chemical shifts in the carbonyl core (C 1s, O 1s) $\rightarrow \pi^*_{C=O}$ transition energy for a series of models containing the carbonyl group (see Scheme 2). We have grouped these models to identify the different carbonyl group environ-

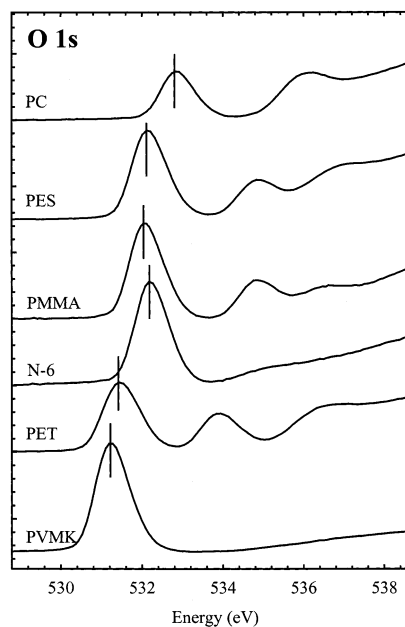


Figure 2. O 1s NEXAFS spectra of polycarbonate (PC), poly(ethylene succinate) (PES), poly(methyl methacrylate) (PMMA), nylon-6 (N6), poly(ethylene terephthalate) (PET), and poly(vinyl methyl ketone) (PVMK). Structures of these polymers are presented in Scheme 1.

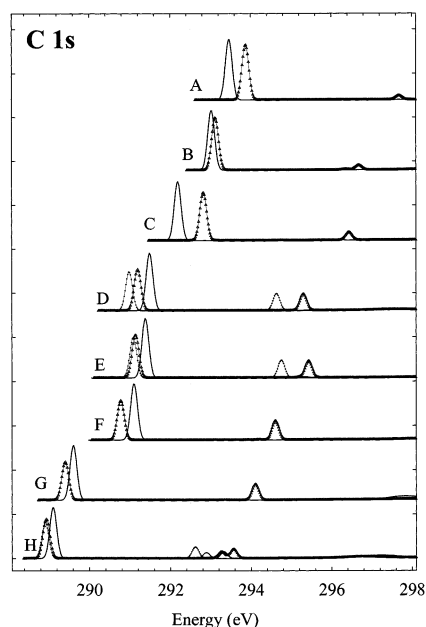


Figure 3. Simulated C 1s NEXAFS spectra of the C 1s (C=O) $\rightarrow \pi^*_{C=O}$ transition for molecular models based on the following motifs: carbonate (A), carbamate (urethane) (B), urea (C), acetate (D), carboxyl (E), amide (F), ketone (G), and aldehyde (H). The aliphatic models are shown in solid lines; the aromatic models in lines with points. The details of the calculations are presented in the text, the energies of the transitions are presented in Table 2, and structures of the molecular models are presented in Scheme 2.

ments, from carbonate (A) to aldehyde (H). For each group, we consider a simple aliphatic model (A1, B1) and at least one aromatically substituted model (A2, B2, etc). For example, for the carbonyl group in a urea linkage (C), we have considered urea (C1) and diphenylurea (C2). Simulations of the ab initio calculations for the C 1s and O 1s NEXAFS spectra of these models are presented in Figures 3 and 4, respectively. Calculated ionization energies, excitation energies, term values and oscillator strengths for the carbonyl core (C 1s, O 1s) $\rightarrow \pi^*_{C=O}$ transition are presented in Table 2.

TABLE 2: Calculated Ionization Potentials, Term Values, Excitation Energies and Oscillator Strengths for the C 1s $\rightarrow \pi^*_{\text{C=O}}$ and O 1s Excitation $\rightarrow \pi^*_{\text{C=O}}$ Excitation in Carbonyl Containing Molecules

molecule	carbon 1s				oxygen 1s			
	IP, eV	TV, ^a eV	energy, eV	Osc	IP, eV	TV, ^a eV	energy, eV	Osc
A1 dimethyl carbonate	297.62	4.16	293.46	0.0733	537.58	3.17	534.41	0.0130
A2 diphenyl carbonate	297.79	3.91	293.87	0.0663	537.53	3.03	534.49	0.0116
B1 ethyl carbamate	296.79	3.76	293.02	0.0727	536.81	2.56	534.25	0.0119
B2 ethyl <i>N</i> -phenyl carbamate	296.63	3.51	293.12	0.0634	536.60	2.46	534.14	0.0095
C1 urea	296.28	4.10	292.19	0.0714	536.61	2.74	533.87	0.1157
C2 diphenyl urea	295.90	3.08	292.82	0.0579	536.11	2.15	533.95	0.0085
D1 methyl acetate	296.01	4.52	291.49	0.0698	537.27	3.86	533.41	0.0146
D2 methyl benzoate	295.70	4.50	291.19	0.0500	536.74	3.96	532.78	0.0087
D3 dimethyl terephthalate	295.87	4.89	290.98	0.0473	536.83	4.38	532.46	0.0078
E1 acetic acid	296.52	5.15	291.37	0.0715	537.70	4.40	533.29	0.0149
E2 benzoic acid	296.11	4.97	291.14	0.0515	537.06	4.35	532.71	0.0087
E3 terephthalic acid	296.40	5.32	291.08	0.0485	537.36	4.78	532.58	0.0082
F1 acetamide	295.27	4.18	291.10	0.0677	536.39	3.29	533.01	0.0126
F2 benzamide	295.05	4.28	290.77	0.0471	535.97	3.62	532.35	0.0071
G1 acetone	294.42	4.81	289.60	0.0658	537.06	4.59	532.48	0.0170
G2 benzophenone	293.93	4.53	289.40	0.0459	536.11	4.26	531.85	0.0094
H1 acetaldehyde	294.75	5.64	289.11	0.0617	537.67	5.50	532.16	0.0180
H2 benzaldehyde	294.31	5.34	288.97	0.0466	536.93	5.21	531.72	0.0110
H3 terephthaldehyde	294.63	5.71	288.91	0.0438	537.17	5.52	531.65	0.0103

^a Term value: energy relative to the ionization potential (excitation energy = IP - TV).

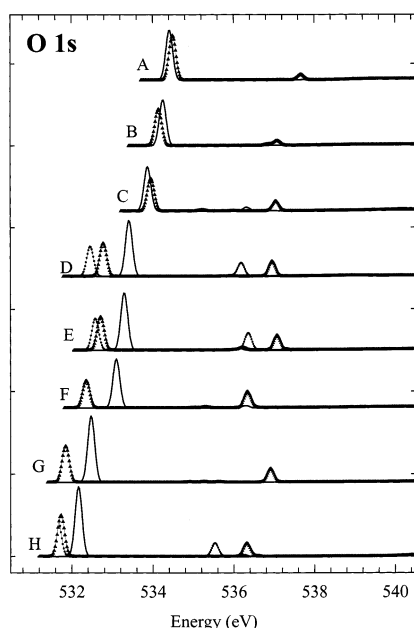


Figure 4. Simulated O 1s NEXAFS spectra of the O 1s (C=O) $\rightarrow \pi^*_{\text{C=O}}$ transition for molecular models based on the following motifs: carbonate (**A**), carbamate (urethane) (**B**), urea (**C**), acetate (**D**), carboxyl (**E**), amide (**F**), ketone (**G**), and aldehyde (**H**). The aliphatic models are shown in solid lines, the aromatic models in lines with points. The details of the calculations are presented in the text, the energies of the transitions are presented in Table 2, and structures of the molecular models are presented in Scheme 2.

These calculations reproduce the experimentally observed trend in the carbonyl core (C 1s, O 1s) $\rightarrow \pi^*_{\text{C=O}}$ transition energy with changes in the carbonyl group bonding environment. We will first focus on two models that are expected to be good molecular models for the C 1s $\rightarrow \pi^*_{\text{C=O}}$ transition energy in two polymers: PC (**A2**, diphenyl carbonate) and PVMK (**G1**, acetone). The ab initio calculations overestimate the energy of the C 1s $\rightarrow \pi^*_{\text{C=O}}$ transition by 3.47 eV for PC and 3.0 eV for PVMK. In the IVO approximation, term values for valence transitions are overestimated since the frozen ion core over-screens the core hole.²⁷ The nature of these differences will be explored below.

An examination of the calculated term values, transition energies, and ionization potentials in Table 2 illustrates the origin

of these chemical shifts. The higher energy core $\rightarrow \pi^*_{\text{C=O}}$ transitions (i.e., **A1**, **A2**) have both smaller term values and higher ionization potentials than the core $\rightarrow \pi^*_{\text{C=O}}$ transitions that occur at lower energies (i.e., **G1**, **G2**). In these C 1s spectra, the range (ΔE) in the calculated ionization potentials (3.48 eV) is greater than the range of the calculated term values (2.13 eV). The reverse is true in the O 1s spectra. The range in calculated ionization potentials (1.6 eV) is smaller than the range of calculated term values (3.35 eV). This result indicates that atomic charge (as reflected in the ionization potential) and the valence electronic structure (as reflected in the term value) both play an important role in defining the chemical sensitivity of this transition, but with different magnitudes at the C 1s and O 1s core edges. It should not be surprising that ionization potential differences are more important in the C 1s spectra than in the O 1s spectra, as the differences in bonding between the carbonyl motifs (**A**, **B**, etc.) are located directly to the carbon atom.

Effect of Aromatic Substitution. The calculated energies of the carbonyl core (C 1s, O 1s) $\rightarrow \pi^*_{\text{C=O}}$ transitions for the aromatic substituted carbonyl structures (dotted lines in Figures 3 and 4) differ from those calculated for the aliphatic species (solid lines in Figures 3 and 4). In the C 1s spectra (Figure 3), the carbonyl C 1s $\rightarrow \pi^*_{\text{C=O}}$ transition shifts to lower energy for motifs **D** through **H** and to higher energy for motifs **A** through **C**. The effect is similar in the O 1s data. This change in the carbonyl core (C 1s, O 1s) $\rightarrow \pi^*_{\text{C=O}}$ transition energy with aromatic substitution suggests the existence of strong bond–bond interactions between the phenyl π^* density and the carbonyl π^* density. The nature of this mixing depends on the term value of the carbonyl π^* , which decreases from motif **A** to motif **H**. This mixing is stronger for motifs **D–H**, where the phenyl group is bonded directly to the carbonyl group, and weaker for motifs **A–C**, where another atom (N or O) forms a “spacer” between the phenyl and the carbonyl group. This form of phenyl/carbonyl π^* conjugation has been discussed previously for substitution isomers of PET.¹⁸

The calculated oscillator strengths for the core (C 1s, O 1s) $\rightarrow \pi^*_{\text{C=O}}$ transitions are presented in Table 2. We note that the oscillator strength for this transition is attenuated when the carbonyl motif (**A–H**) is functionalized by a phenyl group (i.e., 0.0734 for dimethyl carbonate versus 0.0663 for diphenyl carbonate). This decrease in the $\pi^*_{\text{C=O}}$ transition intensity with aromatic substitution is systematic at both the C 1s and the O

TABLE 3: Experimental Excitation Energies for the Carbonyl Core (C 1s, O 1s) $\rightarrow \pi^*_{\text{C=O}}$ Transition in Molecules and Polymers Containing the Carbonyl Group

species	carbon 1s excitation energy, eV		oxygen 1s excitation energy, eV	
	experimental	calculated	experimental	calculated
dimethyl carbonate	290.33 ³⁰	293.46 (A1)	532.93 ³⁰	534.41 (A1)
diphenyl carbonate	290.6 ³⁰	293.87 (A2)		
ethyl carbamate	290.05 ¹²	293.02 (B1)	532.8 ¹²	534.25 (B1)
ethyl <i>N</i> -phenyl carbamate	290.0 ¹²	293.12 (B2)	532.5 ¹²	534.14 (B2)
urea	289.53 ¹²	292.19 (C1)	532.5 ¹²	533.87 (C1)
diphenyl urea	289.4 ¹²	292.82 (C2)	532.5 ¹²	533.95 (C2)
ethyl benzoate	288.2 ²⁹	291.19 (D2)	531.5 ²⁹	532.78 (D2)
poly(ethylene terephthalate)	288.15 ^a	290.98 (D3)		
dimethyl terephthalate			531.5 ¹⁸	532.46 (D3)
acetic acid	288.69 ³¹	291.37 (E1)	531.95 ³¹	533.29 (E1)
benzamide	288.09 ³²	290.77 (F2)		
nylon-6	288.2 ^a	291.10 (F2)		
acetone	286.80 ³³	289.60 (G1)	531.3 ³³	532.48 (G1)
poly(vinyl methyl ketone)	286.6 ^a	289.60 (G1)		
acetaldehyde	286.30 ³³	289.11 (H1)	531.14 ³³	532.16 (H1)
benzaldehyde (b)	287.7 ²⁹	288.97 (H2)	531.0 ²⁹	531.72 (H2)
terephthaldehyde (b)	288.2 ²⁹	288.91 (H3)	530.6 ²⁹	531.65 (H3)

^a This work ^b These data excluded from the fit (see text). ^c Fit to the formula: (calculated energy) = slope x (experimental energy) + intercept. C 1s: slope = 1.0767; intercept = -19.1976; $R^2 = 0.9805$. O 1s: slope = 1.2846; intercept = -150.1461; $R^2 = 0.9796$.

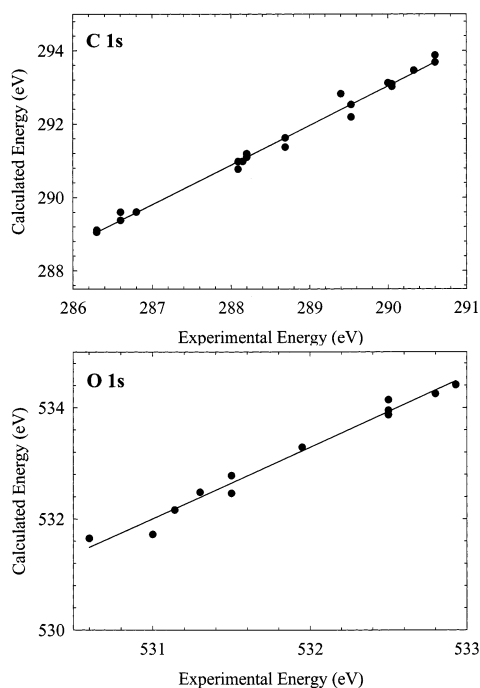


Figure 5. (Top) Plot of the relationship between the calculated and the experimentally measured energy for the C 1s (C=O) $\rightarrow \pi^*_{\text{C=O}}$ transition for a series of molecules containing the carbonyl group (points) and a fit to these data (solid line). These data are fit to the equation $y = mx + b$, with a slope of 1.0767 and an intercept of -19.1976 ($R^2 = 0.9805$). (Bottom) Plot of the relationship between the calculated and the experimentally measured energy for the O 1s (C=O) $\rightarrow \pi^*_{\text{C=O}}$ transition for a series of molecules containing the carbonyl group (points) and a fit to these data (solid line). The calculated and experimental energies are presented in Tables 2 and 3, respectively. These data are fit to the equation $y = mx + b$, with a slope of 1.2846 and an intercept of -150.1461 ($R^2 = 0.9897$).

1s. We also note the prediction of a set of weaker π^* transitions between 292 and 297 eV in the C 1s calculations and 535–537 eV in the O 1s calculations (Figures 3 and 4). The orbital character of these transitions is a core (C 1s, O 1s) $\rightarrow \pi^*_{\text{C=O}}$ transition, formed by conjugation between the phenyl group and the carbonyl group. Similar features have been previously assigned in the spectrum of PET.¹⁸

These calculations serve to illustrate a general point—it is risky to consider the signature of a functional group as an

isolated spectroscopic “fingerprint”. For example, the energy of the core $\rightarrow \pi^*_{\text{C=O}}$ transitions for a carbonate group in one bonding environment may not be the same as for a carbonate group in a similar but different bonding environment (**A1** versus **A2**). Since the absolute energy of the transition appears to be the most important variable for determining the chemical identity, these electronic effects must be carefully considered.

Correlation between Theory and Experiment. The absolute energy of the core (C 1s, O 1s) $\rightarrow \pi^*$ transition energies is needed to assign a transition as originating from a particular type of carbonyl-containing functional group. Experimentally, this requires carefully calibrated spectra. In computational approaches, the IVO approximation overestimates the energy of the predicted core $\rightarrow \pi^*$ transitions. To examine the character of systematic differences between calculations and experiments, we have assembled a large body of experimental and calculated carbonyl core (C 1s, O 1s) $\rightarrow \pi^*$ transition energies. All calculations have been carried out at the same level of theory and we have limited our choice of NEXAFS spectra to those which have been calibrated by using a gas whose energy scale has been precisely measured by inner shell electron energy loss spectroscopy (ISEELS).²⁸

Figure 5 presents the relationship between the calculated and the measured carbonyl core (C 1s, O 1s) $\rightarrow \pi^*_{\text{C=O}}$ transition energies for a series of molecules. The data used for these fits are presented in Table 3. The data show a linear correlation between the experimental and calculated values. In a fit of these data to the equation $y = mx + b$, we find a slope of 1.0767 for the C 1s data ($r^2 = 0.9805$) and a slope of 1.2846 for the O 1s data ($r^2 = 0.9796$). The slope indicates that the difference between calculation and experiment *increases* for features that are located at higher energy, both within a core edge (i.e., C 1s for **A1** versus **H1**) and between core edge spectra (C 1s versus O 1s). This result is consistent with the “stretch” that is observed in NEXAFS spectra calculated by IVO methods.¹⁸

The experimental and calculated energies for the carbonyl C 1s (C=O) $\rightarrow \pi^*_{\text{C=O}}$ transition in benzaldehyde (**H2**) and terephthaldehyde (**H3**)²⁹ were excluded from this analysis as they deviated significantly from the scatter in Figure 5 (top). A feature at 287.7 eV in the gas-phase spectra of these species had been assigned as the carbonyl C 1s (C=O) $\rightarrow \pi^*_{\text{C=O}}$ transition. If we use the fits in Figure 5 to map the calculated energy scale onto the “experimental” energy scale, we could

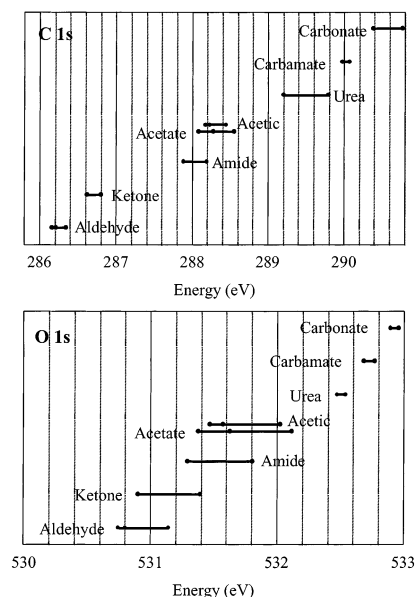


Figure 6. (Top) Spectroscopic correlation diagram for the expected energies of the C 1s $\rightarrow \pi^*_{C=O}$ transitions in molecules containing the carbonyl group. (Bottom) Spectroscopic correlation diagram for the expected energies of the O 1s $\rightarrow \pi^*_{C=O}$ transitions for molecules containing the carbonyl group.

predict that this feature should occur at ~ 286.25 eV. We conclude that the original assignment²⁹ was incorrect and that the carbonyl C 1s ($C=O$) $\rightarrow \pi^*_{C=O}$ transition in benzaldehyde and terephthaldehyde should nearly overlap with the C 1s ($C-R$) $\rightarrow 1\pi^*_{C=C}$ transition. These features could not be resolved in the relatively low resolution ISEELS data (~ 0.7 eV fwhm). This reassignment is also supported by the calculations performed for terephthaldehyde (**H3**) by Pettersson et al.²³

The discovery of this misassignment shows the power of this correlation for future use. We can accurately predict where a specific transition should occur, based on this semiempirical correction of the calculated transition energy scale. This correlation can also be applied to transform the large body of calculated transition energies (Table 2) onto an absolute or "experimental" energy scale. This approach would have great utility for predicting the spectroscopy of short-lived species such as reactive intermediates and side reaction products, where good model spectra would be difficult to obtain but for which calculations are possible.

This semiempirical method corrects for the systematic differences between experiment and theory for the IVO method. The precision of these calculations could be improved by other means, such as use of a larger basis set or advanced methods such as configuration interaction. This relatively simple approach is chosen for its simplicity and its scalability: calculations on larger molecules can be attempted due to the moderate choice of basis set.

We have used the correlation presented in Figure 5 and the body of calculated data in Table 2 to prepare the correlation diagram for the carbonyl core (C 1s, O 1s) $\rightarrow \pi^*_{C=O}$ transition in Figure 6. As a wide range of different structures were sampled, it is quite likely that this correlation diagram represents most of the *potential energy range* for these transitions. The position of these bands in Table 1 is reasonable for known and calibrated experimental data. Given the variability in the transition energy illustrated by this diagram, these "bands" should be viewed as guidelines and not absolute limits. Nevertheless, the development of such correlation diagrams is expected to be very useful for analytical NEXAFS spectroscopy

of organic materials, provided that the energy scale of the analyte spectrum is accurately calibrated.

5. Conclusions

We have recorded the C 1s and O 1s NEXAFS spectra of a variety of polymers where the carbonyl group is present in a range of different chemical environments. The observed trends in the carbonyl core (C 1s, O 1s) $\rightarrow \pi^*_{C=O}$ transitions have been carefully calibrated and were interpreted with the aid of high-quality ab initio calculations. The variation in the core binding energy and the valence (π^*) orbital energies both contribute to the observed chemical shifts. Correlation diagrams have been developed for the carbonyl (C 1s, O 1s) $\rightarrow \pi^*_{C=O}$ transitions, based on calculations for a wide range of species. We expect that these correlation diagrams will be useful for guiding chemical identification using NEXAFS spectroscopy. The need for extensive model spectroscopy studies should be reduced, and the risk of accidental misidentification of overlapping bands reduced. It is essential that the energy scale of the NEXAFS spectra be precisely calibrated, as a small energy miscalibration could be misinterpreted as a chemical shift. Future work will develop the correlation diagrams for the distinctive C 1s ($C-H$) $\rightarrow 1\pi^*_{C=C}$ and the C 1s ($C-R$) $\rightarrow 1\pi^*_{C=C}$ transitions associated with the phenyl ring.

Acknowledgment. Research was carried out at the National Synchrotron Light Source (NSLS) at Brookhaven National Laboratory (supported by the U.S. Department of Energy, Division of Materials Sciences and Division of Chemical Sciences under contract DE-AC02-98CH10886) and at the Synchrotron Radiation Center (SRC) of the University of Wisconsin—Madison (supported by the National Science Foundation under award no. DMR-0084402). C 1s NEXAFS spectra were recorded with the Stony Brook STXM microscope at the NSLS, developed by the group of J. Kirz and C. Jacobsen, with support from the U.S. Department of Energy, Office of Biological and Environmental Research (contract DE-FG02-89ER60858) and the National Science Foundation (grant DBI-9605045). The zone plates for this microscope were developed by S. Spector and C. Jacobsen of Stony Brook and D. Tennant of Lucent Technologies Bell Labs, with support from the NSF under grant ECS-9510499. C 1s NEXAFS spectroscopy was performed by S.G.U. while employed at NCSU. O 1s NEXAFS spectra were recorded on the spherical grating monochromator of the Canadian Synchrotron Radiation Facility (CSRF) at the Synchrotron Radiation Center (SRC). Work was supported in part by NSF Young Investigator Award (DMR-9458060) (H.A., S.G.U.), the National Science and Engineering Research Council—Canada, and the University of Saskatchewan (S.G.U.).

References and Notes

- (1) Ade, H.; Urquhart, S. G. NEXAFS spectroscopy and microscopy of natural and synthetic polymers. In *Chemical Applications of Synchrotron Radiation*; Sham, T. K., Ed.; World Scientific Publishing: River Edge, NJ, 2002.
- (2) Urquhart, S. G.; Hitchcock, A. P.; Smith, A. P.; Ade, H. W.; Lidy, W.; Rightor, E. G.; Mitchell, G. E. *J. Electron Spectrosc. Relat. Phenom.* **1999**, *100*, 119.
- (3) Flynn, G. J.; Keller, L. P.; Midler, M. A.; Jacobsen, C.; Wirick, S. *Lunar Planet. Sci.* **1998**, *XXIX*, Abstr. 1156.
- (4) Flynn, G. J.; Keller, L. P.; Jacobsen, C.; Wirick, S.; Miller, M. A. Organic Carbon in Interplanetary Dust Particles. In *ASP Conference Series 213*, Astronomical Society of the Pacific, 2000, p 191.
- (5) Cody, G. D.; Ade, H.; Anderson, K.; Brandes, J.; Wirick, S., manuscript in preparation.
- (6) Cody, G.; Botto, R. E.; Ade, H.; Wirick, S. *SPIE Proc. Vol.* **1995**, *128*, 185.

- (7) Cody, G. D.; Botto, R. E.; Ade, H.; Behal, S.; Disko, M.; Wirick, S. *Energy Fuels* **1995**, *9*, 525.
- (8) Myneni, S. C. B.; Brown, J. T.; Martinez, G. A.; Meyer-Ilse, W. *Science* **1999**, *286*, 1335.
- (9) Anders, S.; Stammel, T.; Fong, W.; Bogoy, D. B.; Bhatia, C. S.; Stohr, J. J. *Vac. Sci. Technol., A* **1999**, *17*, 2731.
- (10) Kikuma, J.; Tonner, B. P. *J. Electron Spectrosc. Relat. Phenom.* **1996**, *82*, 53.
- (11) Unger, W. E. S.; Lippitz, A.; Wöll, C.; Heckmann, W. *Fresenius' J. Anal. Chem.* **1997**, *358*, 89.
- (12) Urquhart, S. G.; Hitchcock, A. P.; Priester, R. D.; Rightor, E. G. *J. Polym. Sci., Part B: Polym. Phys.* **1995**, *33*, 1603.
- (13) Urquhart, S. G.; Ade, H. W.; Smith, A. P.; Hitchcock, A. P.; Rightor, E. G.; Lidy, W. J. *Phys. Chem. B* **1999**, *103*, 4603.
- (14) Coffey, T. S.; Urquhart, S. G.; Winesett, A. D.; Scholl, A.; Ade, H. *J. Electron Spectrosc. Relat. Phenom.* **2002**, *122*, 65.
- (15) Zhang, X.; Ade, H.; Jacobsen, C.; Kirz, J.; Lindaas, S.; Williams, S.; Wirick, S. *Nucl. Instrum. Methods Phys. Res., Sect. A* **1994**, *347*, 431.
- (16) Ade, H.; Smith, A. P.; Zhang, H.; Zhuang, G. R.; Kirz, J.; Rightor, E.; Hitchcock, A. *J. Electron Spectrosc. Relat. Phenom.* **1997**, *84*, 53.
- (17) Ma, Y.; Chen, C. T.; Meigs, G.; Randall, K.; Sette, F. *Phys. Rev. A* **1991**, *44*, 1848.
- (18) Urquhart, S. G.; Hitchcock, A. P.; Smith, A. P.; Ade, H.; Rightor, E. G. *J. Phys. Chem. B* **1997**, *101*, 2267.
- (19) Kosugi, N.; Kuroda, H. *Chem. Phys. Lett.* **1980**, *74*, 490.
- (20) Hunt, W. J.; Goddard, W. A. I. *Chem. Phys. Lett.* **1969**, *3*, 414.
- (21) Schmidt, M. W.; Baldrige, K. K.; Boatz, J. A.; Elbert, S. T.; Gordon, M. S.; Jensen, J. J.; Koseki, S.; Matsunaga, N.; Nguyen, K. A.; Su, S.; Windus, T. L.; Dupuis, M.; Montgomery, J. A. *J. Comput. Chem.* **1993**, *14*, 1347.
- (22) Huzinaga, S.; Andzelm, J.; Klobukowski, M.; Radzio-Andzelm, E.; Sasaki, Y.; Tatewaki, H. *Gaussian Basis Sets for Molecular Orbital Calculations*; Elsevier: Amsterdam, 1984.
- (23) Pettersson, L. G. M.; Agren, H.; Schürmann, B. L.; Lippitz, A.; Unger, W. E. S. *Int. J. Quantum Chem.* **1997**, *63*, 749.
- (24) Yang, L.; Agren, H.; Carravetta, V.; Pettersson, L. G. M. *Physica Scr.* **1996**, *54*, 614.
- (25) Yang, L.; Agren, H.; Pettersson, L. G. M.; Carravetta, V. *J. Electron Spectrosc. Relat. Phenom.* **1997**, *83*, 209.
- (26) Stener, M.; Lisini, A.; Decleva, P. *Chem. Phys.* **1995**, *191*, 141.
- (27) Kosugi, N., private communication.
- (28) Sohdi, R. N.; Brion, C. E. *J. Electron Spectrosc.* **1984**, *13*, 193.
- (29) Hitchcock, A. P.; Urquhart, S. G.; Rightor, E. G. *J. Phys. Chem.* **1992**, *96*, 8736.
- (30) Hitchcock, A. P.; Wen, A. T.; Urquhart, S. G.; Rightor, E. G., unpublished data, 1991.
- (31) Robin, M. B.; Ishii, I.; McLaren, R.; Hitchcock, A. P. *J. Electron Spectrosc. Relat. Phenom.* **1988**, *47*, 53.
- (32) Urquhart, S. G., unpublished work, **2001**.
- (33) Hitchcock, A. P.; Brion, C. E. *J. Electron Spectrosc. Relat. Phenom.* **1980**, *19*, 231.